Asian Journal of Chemistry; Vol. 34, No. 9 (2022), 2247-2252

ASIAN JOURNAL OF CHEMISTRY

https://doi.org/10.14233/ajchem.2022.23818

Experimental and Quantum Chemical Studies of Induced Liquid Crystal Textures

CH. RAVI SHANKAR KUMAR[1,*], M. PRASANTI[1] and A. JHA[2]

[1]Department of Physics, Institute of Science, GITAM University,Visakhapatnam-530045, India
[2]Department of Chemistry, Institute of Science, GITAM University,Visakhapatnam-530045, India

*Corresponding author: E-mail: rskchaval@gmail.com

Received: 4 March 2022; *Accepted*: 9 May 2022; *Published online*: 19 August 2022; AJC-20917

Dynamics of molecular structures has its dependence on symmetry, topological defects, responsibility to shear, short range interatomic forces, interplay of thermal and potential energies in formation of supramolecular structures with mesophase. Computational studies emerged as sophisticated tool that deliver the functional aspects responsible in formation of these molecular structures. The article attempts induced textures and phase transition studies of synthesized compound from anilines and aldehydes. Infrared spectral studies infer shits in wavenumbers in formation of secondary aldemines with anilines and aldehydes. Polarizing optical microscope and differential scanning calorimetric studies were performed for observation of textures and confirmation of transition temperatures. Computational studies were performed for these compounds responsible for induced phases using 6-311++(d,p) with quantum mechanical descriptors. Studies revealed that reduced energy gap and high dipole moment is consequence of change in order of transition in synthesized compound responsible for induced phase.

Keywords: Quantum chemistry, Smectic B texture, Liquid crystal, Aldemines, Anilines.

INTRODUCTION

Liquid crystalline materials are potential for present day technologies due to their extraordinary structural and physical properties [1,2]. Structural properties depend on control and tuning of organic compound with either liquid crystalline or non-liquid crystalline material leading to discernable change in phase transition and consequently to new phases [3-5]. Charge transfer mechanism is of vital importance due to strong intermolecular interactions that arise due to stiochiometric ratios of mixing between the electron donor and electron acceptor with substantial deviation in respective energies responsible for phase transition, which are thermally stable with induced phases. Studies of liquid crystals [6,7] with mesogenic molecules such as calamatic [8,9], discotic [7,10], banana [11,12], *etc*. Numerous studies associated with mesophases of nematics has its origin from bent core molecules [13,14], banana shaped molecules [15] change in symmetry due to nanoparticles [16], smectics from binary mixtures [17], bent core mesogens [18] and cholesteric phases [19] arising due to self assembly. Reported induced nematic phase [20-23], smectics [24-26] and cholesteric phases [27,28], discotic [26,29,30] and columnar phases [30-32] provides insights to fundamental problems such as phase transitions, defects, growth phenomena, elasticity and optics.

In present day scenario, computational studies concentrated on materials including liquid crystals for its structure and dynamics responsible for self assembly leading to supramolecular structures. Computational studies performed for these liquid crystalline materials hydrogen bonded liquid crystals [33,34], bent core liquid crystals [35], discotic liquid crystals [36], room temperature liquid crystals [37], synthesized liquid crystals [38,39] with spectroscopic properties and induced liquid crystal phases [40,41]. The present focus of work attributes induced phases with synthesized compounds formed from compounds *p*-anisaldehyde and *p*-chloroaniline. Experimental studies confirmed bonding between compounds with infrared spectra, transition temperature and induced phase. Studies responsible for induced phase depend on its structure and associated dynamics were analyzed with quantum mechanical descriptors using DFT method with 6-311++(d,p) basis set.

EXPERIMENTAL

Experimental studies: These studies involve synthesis mechanism, Fourier transform infrared spectroscopy (FTIR),

phase transition studies with differential scanning calorimeter and liquid crystal texture observation using polarizing optical microscope for the non-mesogenic *p*-anisaldehyde (R-2), *p*-chloroaniline (A-2) and synthesized compound (RA-4). The individual compounds were 99% purity obtained form Sigma Aldrich and used as such without further purification.

Synthesis: Green synthesis (ultrasonic assisted synthesis, US) was employed in present study. *p*-Anisaldehyde (R-2, 5 mmol) was dissolved in 10 mL of ethanol and mixed with *p*-chloroaniline (A-2, 5 mmol) also dissolved in 10 mL of ethanol. The solution was sonicated in a probe sonicator (120 mm) with an ultrasonic processor (250 W) operating at a fixed frequency of 50 Hz with speed 238 rpm for 25 min/ 40 min to obtain synthesized compound RA-4 (**Scheme-I**). The reaction content was poured in crushed ice then kept for overnight. The white solid obtained was vacuum filtered and dried to get synthesized compounds with yield of 98%.

Infrared studies: These studies infer changes in wavenumbers in assigned regions of respective characteristic and fingerprint regions analyzed form recorded spectra using FTIR. Infrared spectra was recorded using Thermo Nicolet 6700 spectrophotometer using KBr palette in range 4000-400 cm^{-1} with resolution of 2 cm^{-1}. Interpretation of compounds [42-45] allows necessary changes in respective wavenumbers on abscissa and %transmittance on ordinate. These regions change accordance with molecule as reported in literature [42-45] of spectra with range of wavenumbers in functional and finger print regions for aldehydes and anilines. Range of wavenumbers for aldehydes with assigned stretching modes of C-H (3050-3010); C=C (1600-1475 cm^{-1}), functional group -CHO involves C-H (2900-2700 cm^{-1}), C=O (1700-1660 cm^{-1}) and C-H out-of-plane bend (900-690 cm^{-1}), respectively. Specifically aryl ether (Ar-O-R) group connected to the molecule with the stretching vibrations C-O-C (1040 cm^{-1}) and asymmetric (1250 cm^{-1}) further a methyl group observed at 3000-2840 cm^{-1}.

Corresponding to compound A2 assigned regions of N-H with stretching modes (3500-3300 cm^{-1}), bending (1640-1560 cm^{-1}) and out of plane bend approximately around 800 cm^{-1} with same regions of wavenumbers associated with phenyl ring. The C-N *str*. provides link between phenyl and functional group in range 1350-1000 cm^{-1} in addition to C-Cl *str*. at 785-540 cm^{-1}.

Phase transition studies: Thermal studies were performed in the heating and cooling cycles using differential scanning calorimeter (DSC). DSC studies were carried for compounds with aluminum/platinum crucibles pans at a heating rate of 10 ºC/min in inert atmosphere of nitrogen (30 mL/min). Transition responsible for phase transition; isotropic and crystalline temperatures were recorded with enthalpy during processes between the ranges 40 to 140 ºC [46].

Liquid crystal texture studies: The textures were observed with Olympus BX 51 polarizing optical microscope equipped with heating and cooling stage with LINKAM hot stage at rate of 2º with accuracy of 0.5 ºC. Self assembling of molecules is inherent characteristic responsible for supramolecular structures which arise due to topological defects, change in symmetry and inter atomic forces. These properties are responsible for molecules to shear due to interplay of thermal and potential energies responsible for liquid crystalline texture.

Quantum chemical studies: Quantum chemical calculations include molecular mechanics [47] involving energies at molecular level and electron structure methods [48] with interaction of electrons for deterministic properties. Analysis of molecular structure for physical and chemical properties has its origin in Hartree-Fock theory and density functional theory. Density functional method gained importance for providing inherent phenomena of molecules and attribute related properties responsible for textures. These studies were implemented with Gaussian 16 package Gaussview 6.0 with personal computer using the hybrid three parameter Becke3-Lee-Yang-Parr (B3LYP) method at 298 K with 6-311++(d,p) basis set for all compounds.

RESULTS AND DISCUSSION

Analysis of infrared spectra: Studies of infrared spectra infer the changes in the chemical reaction and molecular geometry arising due to bonding mechanism for formation of synthesized compound. The FTIR spectra of compounds R-2, A-2 and RA-4 are illustrated in Fig. 1.

Analysis of infrared spectra obtained from experimental spectra and computed spectra are approximately similar with the wavenumbers accordingly for compound R2 with the stretching modes can be attributed to C=C (1459 cm^{-1}; 1455 cm^{-1}) of phenyl ring C=O (1689 $^{-1}$; 1639 cm^{-1}) of aldehyde group, twin peaks of C-H of aldehyde group (2843 cm^{-1}; 2743 cm^{-1}; 2879 cm^{-1}), aromatic hydrogen (3050 cm^{-1}; 3013 cm^{-1}; 3075 cm^{-1}) and C-O-C bond having asymmetric stretch (1260 cm^{-1}; 1287 cm^{-1}) and symmetric stretch (1025 cm^{-1}; 1025 cm^{-1}) further out-of-plane bending mode contributing to C-H (833 cm^{-1}; 826 cm^{-1}) of phenyl ring.

Observed primary amino group of compound A-2 at (3468 cm^{-1}; 3571 cm^{-1}) and (3317 cm^{-1}; 3197 cm^{-1}) along with the stretching modes of C-Cl (633 cm^{-1}, 647 cm^{-1}) for chloro group, C=C (1493 cm^{-1}; 1457 cm^{-1}) of phenyl ring, C-N (1283 cm^{-1}; 1299 cm^{-1}) in amine group and out of plane bending mode observed at C-H (825 cm^{-1}; 827 cm^{-1}) of phenyl ring and N-H (825 cm^{-1}, 810 cm^{-1}) of amine group and in plane bending of N-H (1614 cm^{-1}; 1617 cm^{-1}).

Synthesized compound RA4 displayed with stretching modes of C=C (1475 cm^{-1}; 1476 cm^{-1}) in phenyl ring, methyl group (2958 cm^{-1}; 2998 cm^{-1}) C-N (1023 cm^{-1}; 1022 cm^{-1}) and C=N (1608 cm^{-1}; 1643 cm^{-1}) of imine group and C-Cl (540 cm^{-1}; 546 cm^{-1}) for chloro group also C-O-C bond of ether

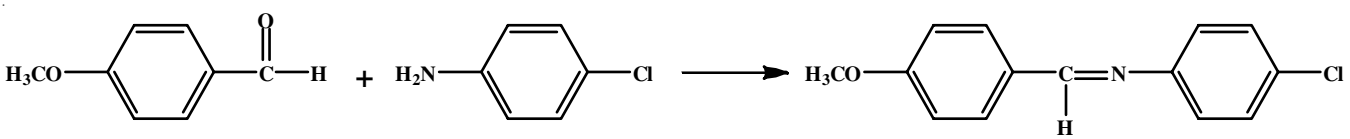

Scheme-I: Ultrasonic synthesis of RA-4

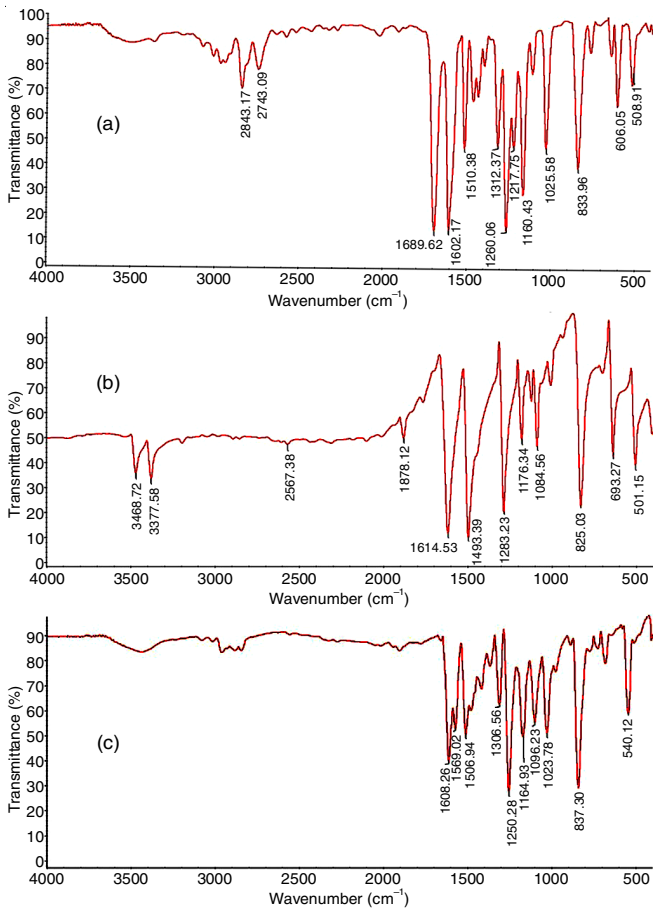

Fig. 1. Infrared spectra of (a) R-2, (b) A-2 and (c) RA-4

show symmetric stretch (1023 cm^{-1}; 1024 cm^{-1}) and asymmetric stretch (1250 cm^{-1}; 1268 cm^{-1}). Out of plane bending mode observed at C-H (836 cm^{-1}; 840 cm^{-1}) of phenyl ring.

Interpretation of the obtained spectra infers that all the wavenumbers of studied compounds are in agreement with reported studies. Moreover, computed spectra inferred no intermediate transitions (no negative wavenumbers and wavenumbers in assigned regions. Prominent changes inferred that the formation of compound RA-4 with significant increase in the wavenumbers of C=C (≅ 15) in phenyl group, methyl group (≅ 115), C-H out of plane bend (≅ 10) corresponding to reduced shifts in asymmetric regions of C-O-C (≅ 15), chloro group (≅ 90) and (≅ 250) corresponding to C-N.

In synthesized compound RA-4, the N-H bonds of aniline at 3468 cm^{-1} and 3317 cm^{-1} as well 1689 cm^{-1} peak for C=O group along with 2843 cm^{-1}, 2743 cm^{-1} of CH of aldehyde group vanished in the process of dehydration during the formation of the new bond C=N in the IR spectrum. During the synthesis process, C=O group of aldehyde group reacts with N-H group of compound A2. As a result, wavenumbers assigned for both the bonds vanished and forms a new bond C=N, which confirms the formation of aldimine. Consequently, shift in assigned wavenumbers of all other bonds were also observed. In other words, the disappearance of CO and CH of aldehyde and amino group of aniline is the clear indication of condensation between compound R2 and compound A2 leading to formation of compound RA-4.

Synthesized molecule RA-4 is a Schiff base compound *i.e.* secondary aldemines [49-52] (R-CH=NR′ where R′ ≠ H) associated with wavenumber regions of both C=N (1690-1640 cm^{-1}) and C-H (2900-2800 cm^{-1}) stretching modes along with phenyl rings. All wavenumbers of computed spectra are in agreement with literature spectra for individuals (R-2, A-2 and RA-4 [53] (Fig. 2).

Phase transition studies: Phase transition studies were studied using DSC, which attribute the transitions from one phase to another phase in heating and cooling cycle with enthalpy. Phase changes are influenced due to changes in enthalpy responsible for short and long range order during transitions. Compound R-2 has no phase transition in heating and associated phase transition at 149.43 ºC with enthalpy 10.51 J/mol in cooling (Fig. 3a). Compound RA-4 has phase transition at 92.5 ºC in heating with enthalpy -28.93 J/mol and in cooling cycle at 60.36 ºC with enthalpy energy of 47.4 J/mol (Fig. 3b).

Liquid crystal textures: Studies with polarizing optical microscope for compound RA-4 has smectic B texture in heating at 88 ºC and schlieren nematic texture at 50 ºC in cooling (Fig. 4) and no texture was observed in compound R-2. Synthesized liquid crystalline mesogen is achiral molecule [54] influenced the positional order with an increase in the molecular length reducing interlayer separation forming smectic B [55-58] texture in heating corresponding to long range order. Large changes enthalpy influenced orientation of neighbouring molecules to shear resulting in schileren nematic droplet texture [59-61] in cooling with short range order.

Quantum chemical calculations: These studies in agreement with the possible explanation from structure aspects to perform experimental studies and explore the hidden molecular properties in terms of optimized ground state energies,

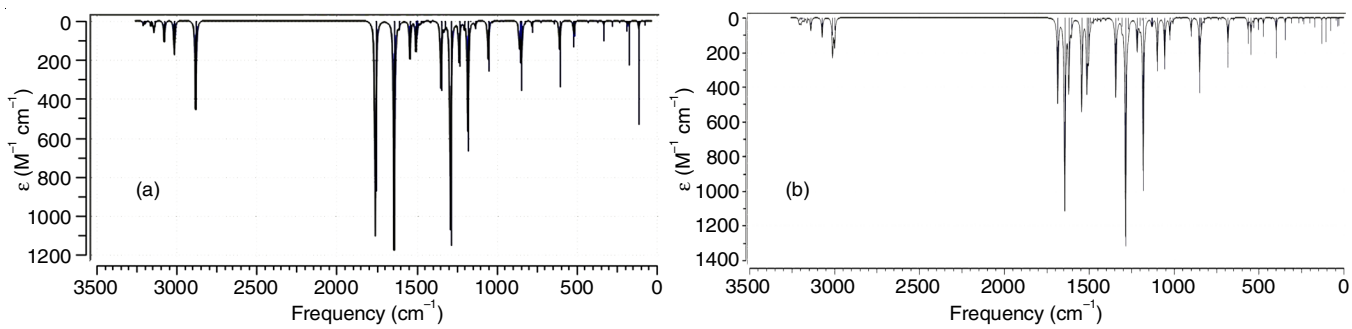

Fig. 2. Computed infrared spectra of (a) R-2 and (b) RA-4

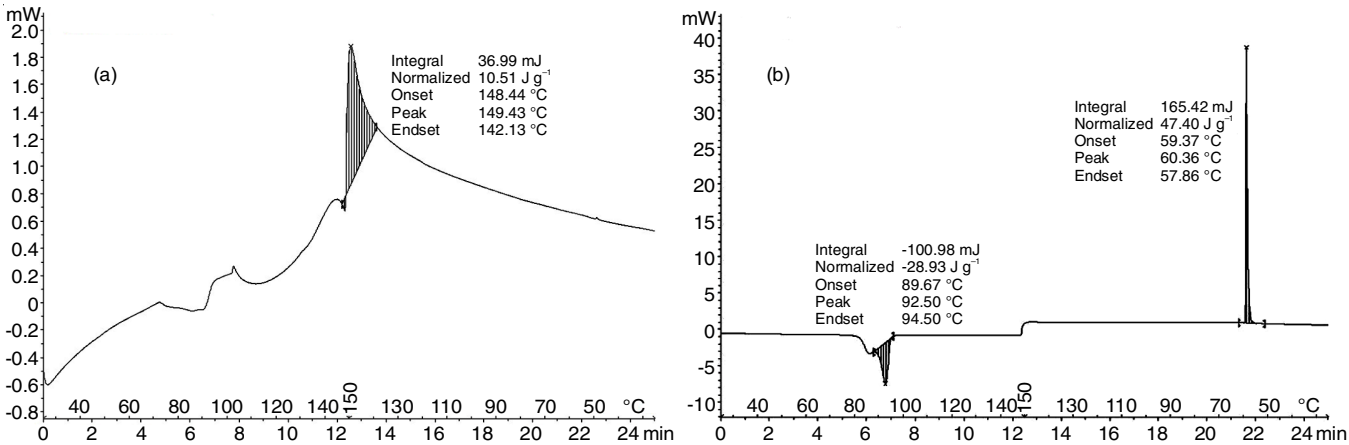

Fig. 3. DSC of (a) R-2 and (b) RA-4

TABLE-1
QUANTUM DESCRIPTORS OF COMPOUNDS

Name of the compound	E_{HOMO} (eV)	E_{LUMO} (eV)	ΔE (eV)	η (eV)	χ (eV)	ω (eV)	μ (Debye)	$\alpha \times 10^{-24}$ (e.s.u.)	$\beta \times 10^{-30}$ (e.s.u.)
R2	-6.733	-1.867	4.866	2.433	4.3	3.799	4.275	15.065	8.561
A2	-5.908	-0.748	5.161	2.580	3.328	2.147	3.519	35.355	0.390
RA4	-6.054	-1.909	4.145	2.072	3.982	3.824	4.302	31.705	8.685

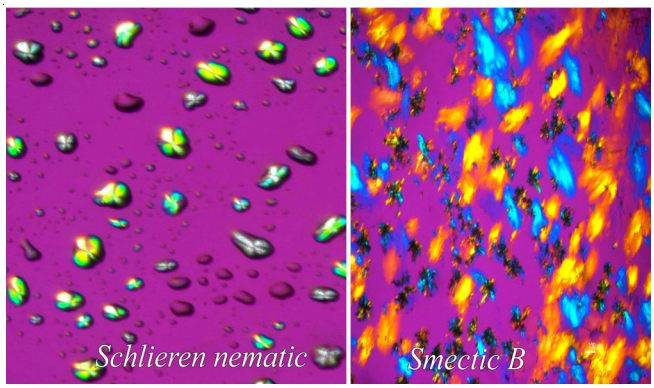

Fig. 4. Observed textures with microscope

transition of states requiring ionization potential, electron affinities, dipole moment and polarization particularly in condensed phases. With Gauss view package the molecular structures were optimized by B3LYP/6-311G++(d,p) method with energy minima corresponding to compound R-2 (-460.228 hartrees), compound A-2 (-747.203 hartrees) and compound RA-4 (-1131.074 hartrees). Electron structure calculations in terms on electron density using Kohn-Sham formulations [62,63] inferred the electronic properties in terms of reactivity of molecule.

Studies of quantum mechanical descriptors [64] indicate that the bonding is spontaneous as energies are negative (Table-1). Quantum descriptors of compounds R-2, A-2 and RA-4 specified that (i) reduction in energy gap enable shear between neighbouring atoms responsible for phase transition; (ii) high kinetic stability responsible for dipole-dipole interactions with enhanced dipole moment; and (iii) reduced hardness (highly soft matter) [34,65] revealed that the synthesized compound RA-4 is liquid crystal mesogen.

Higher electrophilicity index [66] inferred the stabilization of energies with electron transfer between the involved compounds with intermolecular charge transfer in the formation of unique double bond (C=N) responsible for the changes in the polarizability and first order hyperopolarizability with induced phases. Charge transfer [67] mechanism has a significant role in the formation of liquid crystalline compound which enables the neighbouring atoms to alter their order from positional to orientation order (Table-2). Mulliken atomic charges determines the electron population of respective atoms as illustrated in Fig. 5. Studies attributed that the charge transfer arise due to the intermolecular bonding between the involved molecules forming secondary aldemines with induced phases [68,69] in synthesized compound RA-4 with smectic B phase and schlieren nematic texture.

TABLE-2
CHARGE TRANSFER PROPERTIES OF COMPOUNDS

Name of the compound	χ (eV)	μ (eV)	η (eV)	Δn
R-2	4.300	-4.300	2.433	1.767
A-2	3.328	-3.328	2.580	1.289
RA-4	3.982	-3.982	2.072	1.921

Conclusion

Green synthesis mechanism is employed in synthesis of liquid crystalline compound from two non mesogenic compounds. Experimental studies from the recorded infrared spectra attributed the formation of the synthesized compounds with shift in wavenumbers and formation of the secondary aldemine. Phase transition studies indicate the possibility of phase transition in heating and cooling. Induced textures were observed at respective transition temperatures are approximately in

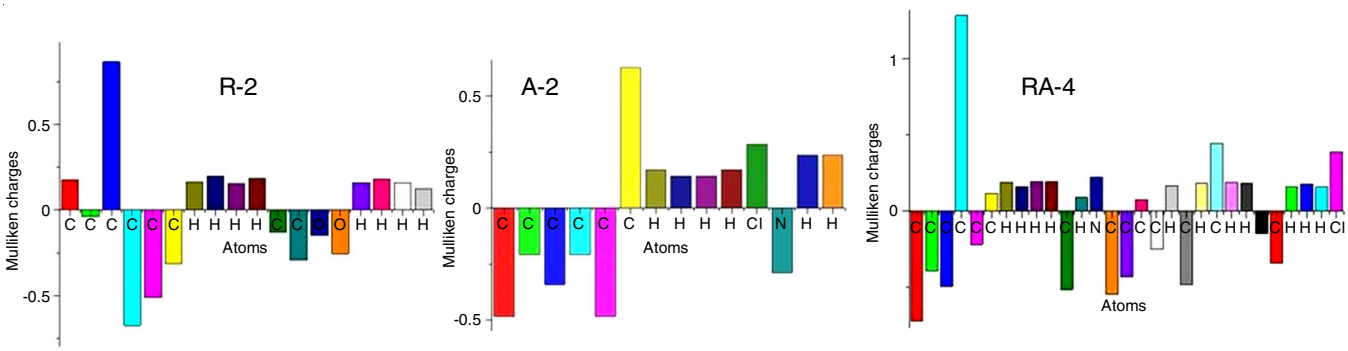

Fig. 5. Mulliken charges of compounds

agreement with phase transition studies. Short range order and long range order are influenced with changes in enthalpy responsible for formation of mesogenic compound. Quantum chemical studies indicated that the wavenumbers were in agreement with the experimental spectra and possible explanation with reduced energy gap, hardness and enhanced dipole moment responsible for induced texture.

ACKNOWLEDGEMENTS

The authors acknowledge to Spectroscopy Analytical Test Facility, I.I.S.C. Bangalore, India for recording the infrared, DSC and optical textures. The authors also thank the support extended by the Department of Chemistry (DST-FIST), Department of Physics (DST-FIST) and Government of India for the technical support of Gaussian package.

CONFLICT OF INTEREST

The authors declare that there is no conflict of interests regarding the publication of this article.

REFERENCES

1. S. Mohanty, *Resonance*, **8**, 52 (2003); https://doi.org/10.1007/BF02837958
2. D. Andrienko, *J. Mol. Liq.*, **267**, 520 (2018); https://doi.org/10.1016/j.molliq.2018.01.175
3. M. Schadt, *Annu. Rev. Mater. Sci.*, **27**, 305 (1997); https://doi.org/10.1146/annurev.matsci.27.1.305
4. S. Tantrawong, *Mater. Today*, **17**, 147 (2014); https://doi.org/10.1016/j.mattod.2014.03.001
5. M. Castillo-Vallés, A. Martínez-Bueno, R. Giménez, T. Sierra and M.B. Ros, *J. Mater. Chem. C Mater. Opt. Electron. Devices*, **7**, 14454 (2019); https://doi.org/10.1039/C9TC04179F
6. J. Uchida, B. Soberats, M. Gupta and T. Kato, *Adv. Mater.*, **34**, 2109063 (2022); https://doi.org/10.1002/adma.202109063
7. N.A. Razali and Z. Jamain, *Polymers*, **13**, 3462 (2021); https://doi.org/10.3390/polym13203462
8. J. Szydlowska, A. Krówczyński, E. Górecka and D. Pociecha, *Soft Matter*, **15**, 7195 (2019); https://doi.org/10.1039/C9SM01080G
9. J. Han, X.-Y. Chang, L.-R. Zhu, Y.-M. Wang, J.-B. Meng, S.-W. Lai and S.S.-Y. Chui, *Liq. Cryst.*, **35**, 1379 (2008); https://doi.org/10.1080/02678290802617724
10. S.-Y. Fan, H.-T. Xu, Q.-G. Li, D.-M. Fang, W.-H. Yu, S.-K. Xiang, P. Hu, K.-Q. Zhao, C. Feng and B.-Q. Wang, *Liq. Cryst.*, **47**, 1041 (2020); https://doi.org/10.1080/02678292.2019.1704898
11. S. Umadevi and B.K. Sadashiva, *Liq. Cryst.*, **32**, 287 (2005); https://doi.org/10.1080/02678290500031814
12. X. Ma and E. Tjhung, *Phys. Rev. E*, **100**, 012701 (2019); https://doi.org/10.1103/PhysRevE.100.012701
13. A. Jákli, *Liq. Cryst. Rev.*, **1**, 65 (2013); https://doi.org/10.1080/21680396.2013.803701
14. J. Matraszek, J. Mieczkowski, J. Szydlowska and E. Gorecka, *Liq. Cryst.*, **27**, 429 (2000); https://doi.org/10.1080/026782900202895
15. H.F. Gleeson, S. Kaur, V. Görtz, A. Belaissaoui, S. Cowling and J.W. Goodby, *ChemPhysChem*, **15**, 1251 (2014); https://doi.org/10.1002/cphc.201400014
16. M. Krasna, M. Cvetko and M. Ambrozic, *Beilstein J. Org. Chem.*, **6**, 74 (2010); https://doi.org/10.3762/bjoc.6.74
17. N. Kapernaum, F. Knecht, C.S. Hartley, J.C. Roberts, R.P. Lemieux and F. Giesselmann, *Beilstein J. Org. Chem.*, **8**, 1118 (2012); https://doi.org/10.3762/bjoc.8.124
18. V. Prasad, S.-W. Kang, K.A. Suresh, L. Joshi, Q. Wang and S. Kumar, *J. Am. Chem. Soc.*, **127**, 17224 (2005); https://doi.org/10.1021/ja052769n
19. M. Mitov, *Soft Matter*, **13**, 4176 (2017); https://doi.org/10.1039/C7SM00384F
20. S.K. Sarkar and M.K. Das, *Phase Transit.*, **89**, 910 (2016); https://doi.org/10.1080/01411594.2015.1106540
21. L. Abdullah Alshabanah, L.A. Al-Mutabagani, H.A. Ahmed and M. Hagar, *Molecules*, **25**, 1694 (2020); https://doi.org/10.3390/molecules25071694
22. V.A. Burmistrov, I.V. Novikov, V.V. Aleksandriiskii, M.K. Islyaikin, A.S. Kuznetsova and O.I. Koifman, *J. Mol. Liq.*, **287**, 110961 (2019); https://doi.org/10.1016/j.molliq.2019.110961
23. K. Kaneko, M. Goto, Y. Haketa, H. Maeda and T. Hanasaki, *Chem. Lett.*, **47**, 1180 (2018); https://doi.org/10.1246/cl.180509
24. A. Knezeviæ, I. Dokli, M. Sapunar, S. Šegota, U. Baumeister and A. Lesac, *Beilstein J. Nanotechnol.*, **9**, 1297 (2018); https://doi.org/10.3762/bjnano.9.122
25. S. Sundaram, P. Subhasri, T.R. Rajasekaran, R. Jayaprakasam, T.S. Senthil and V.N. Vijayakumar, *Ferroelectrics*, **510**, 103 (2017); https://doi.org/10.1080/00150193.2017.1328245
26. W.-R. Chen, C.-M. Chen, J.-C. Hwang and B.-R. Liaw, *Jpn. J. Appl. Phys.*, **44(5A)**, 3126 (2005); https://doi.org/10.1143/JJAP.44.3126
27. I. Dierking, F. Gieâelmann, P. Zugenmaier, W. Kuczynskit, S.T. Lagerwall and B. Stebler, *Liq. Cryst.*, **13**, 45 (1993); https://doi.org/10.1080/02678299308029052
28. M. Bagnani, P. Azzari, S. Assenza and R. Mezzenga, *Sci. Rep.*, **9**, 12654 (2019); https://doi.org/10.1038/s41598-019-48996-3
29. T. Wöhrle, I. Wurzbach, A. Kostidou, N. Kapernaum, J. Litterscheidt, J. Kirres, J.C. Haenle, P. Staffeld, A. Baro, F. Giesselmann and S. Laschat, *Chem. Rev.*, **116**, 1139 (2016); https://doi.org/10.1021/acs.chemrev.5b00190
30. O. Cienega-Cacerez, C. García-Alcántara, J.A. Moreno-Razo, E. Díaz-Herrera and E.J. Sambriski. *Soft Matter*, **12**, 1295 (2016); https://doi.org/10.1039/C5SM01959A

31. B.-H. Tan, M. Yoshio and T. Kato, *Chem. Asian J.*, **3**, 534 (2008); https://doi.org/10.1002/asia.200700225
32. R.-T. Wan, S.-J.J. Tsai, G.-H. Lee and C.K. Lai, *Dyes Pigments*, **173**, 107913 (2020); https://doi.org/10.1016/j.dyepig.2019.107913
33. S. Sundaram, R. Jayaprakasam, M. Dhandapani, T.S. Senthil and V.N. Vijayakumar, *J. Mol. Liq.*, **243**, 14 (2017); https://doi.org/10.1016/j.molliq.2017.08.010
34. H.A. Ahmed, M. Hagar and O.A. Alhaddad, *Crystals*, **9**, 133 (2019); https://doi.org/10.3390/cryst9030133
35. D. Bhattacharjee, T.K. Devi, R. Dabrowski and A. Bhattacharjee, *J. Mol. Liq.*, **272**, 239 (2018); https://doi.org/10.1016/j.molliq.2018.09.052
36. M.S. Mahmood, S. Mohd Said, A. Chatterjee, M.F.M. Sabri, A. Mainal, M.N. Daud and N.A. Sairi, *Mater. Res. Express*, **5**, 126306 (2018); https://doi.org/10.1088/2053-1591/aae11d
37. D.K. Shukla, V.S. Sharma, V. Prajapat and R.B. Patel, *Mol. Cryst. Liq. Cryst.*, **682**, 8 (2019); https://doi.org/10.1080/15421406.2019.1641981
38. D. Sharma and S.N. Tiwari, *Emerg. Mater. Res.*, **6**, 322 (2017); https://doi.org/10.1680/jemmr.15.00052
39. A.K.-T. Mohammad, R.Y. Alwari, H.T. Srinivasa, S.M.H. Al-Majidi and O.I. Alajrawy, *Liq. Cryst.*, **45**, 1699 (2018); https://doi.org/10.1080/02678292.2018.1475685
40. S. Prasad and D.P. Ojha, *Am. J. Mater. Sci.*, **7**, 35 (2017).
41. P. Subhasri, R. Jayaprakasam and V.N. Vijayakumar, *Int. J. Mod. Phys. B*, **32**, 1850223 (2018); https://doi.org/10.1142/S0217979218502235
42. L.P. Donald, G.L. Lampman, G.S. Kriz and J.R. Vyvyan, Introduction to Spectroscopy, Cengage Learning: Stanford, USA, Ed. 5 (2015).
43. R.M. Silverstein, F.X. Webster, D.J. Kiemle and D.L. Bryce, Spectrometric Identification of Organic Compounds, John Wiley & Sons: USA, Ed.: 8 (2007).
44. E. Pretsch, P. Buhlmann and M. Badertscher. Structure Determination of Organic Compounds, Springer-Verlag: Berlin Heidelberg, Fourth Revised and Enlarged Edition (2009)
45. L.D. Field, S. Sternhell and R. Kalman, Organic Structures from Spectra, John Wiely & Sons: England (2008).
46. P. Gill, T.T. Moghadam and B. Ranjbar, *J. Biomol. Technol.*, **21**, 167 (2010).
47. N.L. Allinger, X. Zhou and J. Bergsma, *J. Mol. Struct. THEOCHEM*, **312**, 69 (1994); https://doi.org/10.1016/S0166-1280(09)80008-0
48. W. Andreas, Götz Electronic Structure Calculations on Graphics Processing Units: From Quantum Chemistry to Condensed Matter Physics, Chap. 3: Overview of Electronic Structure Methods, John Wiley & Sons Ltd. (2016).
49. D.L. Pavia, G.M. Lampman and G.S. Kriz, Introduction to Spectroscopy Brooks/Cole CENGAGE Learning: Washington, USA, pp. 31-84 (2009).
50. S. Chakraborty, G. Leitus and D. Milstein, *Angew. Chem.*, **56**, 2074 (2017); https://doi.org/10.1002/anie.201608537
51. K. Tabei and E. Saitou, *Bull. Chem. Soc. Jpn.*, **42**, 1440 (1969); https://doi.org/10.1246/bcsj.42.1440
52. S. Shahab, M. Sheikhi, L. Filippovich, D.E. Anatol'evich and H. Yahyaei, *J. Mol. Struct.*, **1137**, 335 (2017); https://doi.org/10.1016/j.molstruc.2017.02.056
53. J. Spanget-Larsen, Infrared Intensity and Lorentz Epsilon Curvefrom Gaussian FREQ Output, Roskilde University Chemistry (2015).
54. J.P. Abberley, R. Killah, R. Walker, J.M.D. Storey, C.T. Imrie, M. Salamończyk, C. Zhu, E. Gorecka and D. Pociecha, *Nat. Commun.*, **9**, 228 (2018); https://doi.org/10.1038/s41467-017-02626-6
55. Y. Yamamura, T. Murakoshi, S. Iwagaki, N. Osiecka, H. Saitoh, M. Hishida, Z. Galewski, M. Massalska-Arodz and K. Saito, *Phys. Chem. Chem. Phys.*, **19**, 19434 (2017); https://doi.org/10.1039/C7CP03863A
56. N. Osiecka, A. Budziak, Z. Galewski and M. Massalska-Arodz, *Phase Transit.*, **85**, 314 (2012); https://doi.org/10.1080/01411594.2011.646268
57. P.J. Repasky, D.M. Agra-Kooijman, S. Kumar and C.S. Hartley, *J. Phys. Chem. B*, **120**, 2829 (2016); https://doi.org/10.1021/acs.jpcb.5b10990
58. S. Singh, Liquid Crystals Fundamentals, World Scientific Publishing Co. Pvt. Ltd.: Singapore (2002).
59. M.A. Qaddoura and K.D. Belfield, *Int. J. Mol. Sci.*, **10**, 4772 (2009); https://doi.org/10.3390/ijms10114772
60. A.M. Parshin, V.A. Gunyakov, V.Y. Zyryanov and V.F. Shabanov, *Int. J. Mol. Sci.*, **14**, 16303 (2013); https://doi.org/10.3390/ijms140816303
61. J. Nehring and A. Saupe, *J. Chem. Soc., Faraday Trans. II*, **68**, 1 (1972); https://doi.org/10.1039/F29726800001
62. W. Kohn and L.J. Sham, *Phys. Rev.*, **140(4A)**, A1133 (1965); https://doi.org/10.1103/PhysRev.140.A1133
63. A. Klein and R.M. Dreizler, *Phys. Rev. A*, **58**, 1581 (1998); https://doi.org/10.1103/PhysRevA.58.1581
64. V. Balakrishnan and P.M. Andavan, *Elixir Vib. Spec.*, **43**, 7044 (2012).
65. S. Senthan, S. Srinivasan and S. Kabilan, *Mol. Cryst. Liq. Cryst.*, **609**, 249 (2015); https://doi.org/10.1080/15421406.2014.963210
66. S. Prasad and D.P. Ojha, *Mol. Cryst. Liq. Cryst.*, **658**, 69 (2017); https://doi.org/10.1080/15421406.2017.1415656
67. J. Padmanabhan, R. Parthasarathi, V. Subramanian and P.K. Chattaraj, *J. Phys. Chem. A*, **111**, 1358 (2007); https://doi.org/10.1021/jp0649549
68. V. Thangavel, B. Venkataraman, S. Prakasan, J. Ramasamy and V.V. Nallagounder, *Braz. J. Phys.*, **50**, 39 (2020); https://doi.org/10.1007/s13538-019-00724-y
69. P. Upadhyay, M.K. Rastogi and D. Kumar, *Chem. Phys.*, **456**, 41 (2015); https://doi.org/10.1016/j.chemphys.2015.03.011